2024-01-2548 Published 09 Apr 2024

A Drag-Reduction Prediction Model for Truck Platoons

Brian McAuliffe National Research Council Canada

Citation: McAuliffe, B., "A Drag-Reduction Prediction Model for Truck Platoons," *SAE Int. J. Advances & Curr. Prac. in Mobility* 7(1):153-167, 2025, doi:10.4271/2024-01-2548.

This article was presented at the WCX SAE World Congress Experience, April 16-18, 2024.

Received: 27 Oct 2023 Revised: 21 Dec 2023 Accepted: 19 Jan 2024

Abstract

Truck platooning is an emerging technology that exploits the drag reduction experienced by bluff bodies moving together in close longitudinal proximity. The drag-reduction phenomenon is produced via two mechanisms: wake-effect drag reduction from leading vehicles, whereby a following vehicle operates in a region of lower apparent wind speed, thus reducing its drag; and base-drag reduction from following vehicles, whereby the high-pressure field forward of a closely-following vehicle will increase the base pressure of a leading vehicle, thus reducing its drag.

This paper presents a physics-guided empirical model for calculating the drag-reduction benefits from truck platooning. The model provides a general framework from which the drag reduction of any vehicle in a heterogeneous truck platoon can be calculated, based on its isolated-vehicle drag-coefficient performance and limited geometric considerations. The model is adapted from others that predict the influence of inter-vehicle distance for vehicle platoons, but extends the concept to account for cross winds and for lateral offsets between sequential vehicles, thus permitting its use for a range of modelling and simulation applications. Good agreement with experimental data sets from wind-tunnel and track tests is demonstrated in the paper.

Introduction

Heavy-truck platooning is an emerging technology that exploits the drag reduction experienced by bluff bodies moving together in close longitudinal proximity. Numerous studies have examined truck platooning from the perspectives of drag-reduction and fuel economy, as summarized by McAuliffe and Ahmadi-Baloutaki [1], and more recently by Törnell et al. [2]. The drag-reduction phenomena are produced via two general mechanisms: 1) base-drag reduction from following vehicles, whereby the high-pressure field forward of a closely-following vehicle will increase the base pressure of a leading vehicle, thus reducing its drag; and 2) wake-effect drag reduction from leading vehicles, whereby a following vehicle operates in a region of lower relative wind speed, thus reducing its drag.

The aerodynamic benefits of truck platooning are quantified, most often, through testing or simulation, making use of field measurements on open roads or test tracks, scaled-model wind-tunnel testing, or computational fluid dynamics (CFD) simulations. Each of these methods has its benefits and deficiencies, but they all require extensive resources. Such evaluations provide measures of drag reduction or energy savings for an ideal platoon that can be sustained indefinitely, and specific to the truck configurations or platoon formations evaluated. In recent years, there has been a proliferation of economic analyses of truck platooning that consider usage influences such as technology penetration rates, driver preferences, freight networks, and costs (ex. [3, 4]). On the vehicle-technology front, realistic environmental factors such as grades and traffic behaviours (acceleration/braking events) have been examined in the context of limitations they impose on achieving maximum benefits (ex. [5]). These economic and energy-use studies generally assume a simple performance benefit associated with truck platooning, often based on the published performance of an ideal platoon scenario (for example, 10% fuel savings regardless of platoon configuration or duty cycle). To enhance such analyses with realistic performance prediction, simplified aerodynamic models are sought. Two such models have been published in recent years, that provide opportunities for efficient analytical quantification, while providing the potential to examine changing aerodynamic benefits based on platoon configuration.

Tadakuma et al. [6] present a general aerodynamic model of road-vehicle platooning for any number of

© 2024 National Research Council Canada; Published by SAE International. This Open Access article is published under the terms of the Creative Commons Attribution License (http://creativecommons.org/licenses/by/4.0/), which permits distribution, and reproduction in any medium, provided that the original author(s) and the source are credited.

vehicles, based on data for light-duty vehicles, that accounts for separation distance, relative vehicle size, and lateral offset. Schmid et al. [7] adapted components of the model of Tadakuma et al. for truck platooning and used fuel-economy data for model tuning and validation. Both of these models address base-drag reduction using a curve-fitting approach, while employing empirically-tuned wake-decay models for wake-effect drag reduction. These models provide reasonable prediction of drag reduction based on truck position in the platoon and separation distance, but do not account for cross winds which can have a measurable influence on aerodynamic benefits [1, 8, 9]. Tadakuma et al. account for lateral offsetting within the wake and differences in vehicle size, but Schmid et al., whose model is specific to trucks for which cross winds have a greater influence than for passenger vehicle, do not. Sujan et al. [10] also describe a model developed to represent current and next-generation heavy-truck aerodynamic performance, but their model appears to be a curve-fit approach based on drag-reduction data estimated from fuel-savings data. The model of Sujan et al. is therefore limited in its general use because of the assumptions made to convert the results from fuel-savings to drag-reductions (vehicle weights, tire performance, drivetrain efficiency, etc.) and due to the limited configurations on which the curve-fits are based.

With a goal to examine the potential for truck platooning with respect to the specific wind climate in which the vehicles operate, an improved aerodynamic model of truck platooning was developed to account for many real-world factors. The model presented here is based, in part, on similar approaches to those used by Tadakuma et al. [6] and Schmid et al. [7], but has been expanded using physics-based empirical modelling to account for the following influences:

- Any number of trucks in the platoon;
- Separation distance between each truck (same or variable);
- Lateral offset from truck to truck (same or variable);
- Cross winds (up to ±15° yaw angle); and
- Truck configuration (different tractor and trailer configurations).

The sample calculations provided by Schmid et al. could not be replicated by the author due to insufficient documentation of the units or normalizations used to define the empirical coefficients, providing limited use as a basis for comparison.

This paper presents this new aerodynamic-drag-coefficient model for truck platooning. The model was developed from data available for North-American long-nose trucks, but is adaptable for different truck shapes via geometric parameters and specific coefficients, as demonstrated herein by successful application to a cab-over-truck configuration. The data sources upon which the model is based are described first, followed by a description of the model and its components, and subsequent validation against sample data sets.

Source Data

The data sets used to develop the model, and used to improve upon the models of Tadakuma et al. [6] and Schmid et al. [7], are primarily from projects undertaken by the author, with some data supplied by a partner. The data sets, based on chronology of when the experiments were undertaken, are:

1. 1/50-scale Wind-tunnel Aerodynamic-drag Experiments: The US Lawrence Livermore National Laboratory (LLNL) data set, comprised of data collected in 2016 and 2018 in the NASA Ames Army 7-ft × 10-ft Wind Tunnel [8, 11], examined the influence of separation distance (1.5 m to 97 m), number of trucks (2 to 4), lateral offset (up to 1.3 m), and trailer configuration (with side-skirts and an optional boat-tail) on the performance of a platoon comprising a range of tractor configurations and box-van trailer configurations. The author was not involved in this study but the individual C_D values for non-proprietary truck configurations were shared by LLNL. These data were used primarily for model validation.
2. Track Fuel-consumption and Aerodynamic-drag Experiments: Measurements conducted in 2016, 2017 and 2019 at a closed test track examined the influence of separation distance (4 m to 87 m), number of trucks (2 and 3), lateral offset (up to 1.3 m), and trailer configuration (dry-van with/without side-skirts+boat-tail, and a flatbed) [12, 13, 9, 14, 15]. Fuel-savings measurements for all test configurations have been reported, while aerodynamic-drag measurements are only available predominantly from the 2019 2-truck experiments, with some high-uncertainty drag measurements from the 2017 experiments. These data were used for model development and tuning, primarily for large separation distances, greater than about 20 m, and for some cross-wind effects.
3. 1/15-scale Wind-tunnel Aerodynamic-drag Experiments: This data set, acquired in 2017, examined the influence of separation distance (3 m to 22.5 m), lateral offset (up to 3.7 m), trailer configuration (with and without side-skirts and boat-tails), and the presence of a laterally-adjacent passenger vehicles on the performance of a two-truck platoon comprising short-sleeper-cab-tractor with dry-van-trailer configurations [1, 16]. These data were used as the primary data set to develop the model to account for the influences of separation distance, lateral offset, cross winds, and truck configuration.
4. 1/15-scale Wind-tunnel Wake-survey Experiments: Wake-flow-field measurements, acquired in 2019, were used to examine the characteristics of wakes, providing insight and data to model the wake of a heavy truck [17, 18]).
5. 30%-scale Wake-effects Wind-tunnel Experiments: Using a novel wake-generator system, the

influence of upstream traffic on the aerodynamic performance of a 30%-scale truck model was examined. Data representing a truck positioned 50 m and 100 m forward of the test model were acquired and provide large-distance model-validation data that consider yaw angles up to 11° [19].

The model presented in the next section is, in some cases, based directly on the aerodynamic-drag and wake-flow measurements, and in other cases, guided by the observations of these studies. A follow-up adaptation was accommodated based on some limited no-cross-wind high-fidelity CFD data for cab-over trucks by Törnell et al. [2].

Aerodynamic Drag Coefficient Model

The model addresses the relative aerodynamic interaction between vehicles within the platoon, focusing on the two dominant drag-reduction mechanisms:

1. Base-drag reduction from following vehicles; and
2. Wake-effect drag reduction from forward vehicles.

For each vehicle in the platoon, these mechanisms are modelled separately and then combined. Calculations are undertaken in progression from the first vehicle to the last.

The model is based on prescribed reference aerodynamic-drag-coefficient performance of the vehicles that form the platoon. A reference drag-coefficient model is required for each vehicle, whether analytical, empirical, or based on discrete measurements, that defines the variation of drag coefficient with yaw angle, C_{Dref} (ψ). The models developed for each of the two drag-reduction mechanisms were first developed without considering cross winds, defined by the C_{D0} values (= $C_D(0°)$), with cross-wind effects subsequently introduced as an adaptation to the zero-yaw values.

At the outset of the development of the model, consideration was given to developing the model in the frame of reference of the wind vector, due to the desire to model adequately the propagation of the wake in cross winds [20]. Such an approach would require use of a wind-axis drag coefficient as the principal metric, as opposed to the more-commonly-reported body-axis drag coefficient. A wind-axis approach may provide a more general foundation for relating wake deficits to aerodynamic drag, but would limit its use due to the necessity to also consider the side-force coefficients and to transform between the body- and wind-axis coordinate systems. Side-force-coefficient performance is not often documented in published wind-tunnel or CFD studies, and is not a parameter that can be inferred from road/track-test aerodynamic test methods (coast-down or constant-speed). Therefore, a body-axis drag-coefficient approach has been adopted, requiring a greater level of empiricism, but with greater potential for its application and with more validation data accessible.

The source of the reference drag-coefficient data, C_{Dref} (ψ), and it constituent components is important. Contributions due to ground and wheel motion, including ventilation drag, that scale predominantly with ground speed instead of wind speed, should be excluded from the reference values. Data that include ventilation drag, such as field measurements from coast-down/constant-speed methods [15] or from wind-tunnel/CFD simulations that account for it [21], must be adapted before applying this drag-reduction model.

The proposed platoon-drag-reduction model, representing the drag coefficient for truck *n* of a platoon ($C_{D,n}$) operating at a specified freestream yaw angle (ψ_{fs}), is defined as:

$$C_{D,n}\left(\psi_{fs}\right) = \ldots$$
$$\left[1-\left(1-\frac{C_{D0,n}}{C_{D0ref,n}}\right)\left(\frac{\Delta U}{\Delta U_0}\right)^2+\frac{\Delta C_{Dbase,n}}{C_{D0ref,n}}\right]C_{Dref,n}\left(\psi_{eff}\right) \quad (1)$$

This is the core model description, with the sub models for each of its terms described in subsequent sections of this paper. A list of nomenclature describing the symbols and subscripts is found at the end of the paper.

The contents of the square brackets in Equation 1 are analogous to the contents of the drag-reduction-ratio term (*DRR*) used by Tadakuma et al. [6] and by Schmid et al. [7]. Within the square brackets, the wake-effect drag reduction (mechanism 2) is treated via the $C_{D0,n}/C_{D0ref,n}$ term, with a cross-wind and lateral-offset correction applied through the $(\Delta U/\Delta U_0)^2$ term, and the base-drag reduction (mechanism 1) is treated via the $\Delta C_{Dbase,n}/C_{D0ref,n}$ term. The drag-reduction ratio (the contents of the square brackets) is applied to the reference drag-coefficient evaluated at an effective yaw angle, ψ_{eff}, that accounts for the flow structure of the wake under cross-wind conditions.

This new model shares similarities with that of Tadakuma et al. [6], including the use of wake-propagation and wake-shape characteristics to define the sub models. Their model was used initially as the basis for this new model but, as with Schmid et al. [7], differences between light-duty- and heavy-duty-vehicle aerodynamic characteristics, particularly the differences under cross winds, led to modifications and different formulations of the various sub models. The main factors that differentiate this model from that of Tadakuma et al. are:

- The wake-propagation formula make use of the Eskridge and Thompson [20] model, defined for wakes adjacent to a ground plane, that differs from the axisymmetric-wake model employed by Tadakuma et al.;
- A non-normalized form of the base-drag reduction term is used to predict better the effect for heavy trucks;
- A single wake-shape-influence term is used to address close-distance effects, rather than the two-region formulation used by Tadakuma et al.;
- Lateral-offset effects are treated in a separate term in combination with cross-wind effects, instead of

addressing it within a close-distance-correction term; and

- This model is valid to shorter separation distances (about 3 m) compared to that of Tadakuma et al. (10 m).

Due to these differences, direct comparisons of new-model predictions to those from Tadakuma et al. are not presented here. Differences in formulations amongst sub models, and amongst the effects that each addresses, makes such comparisons difficult. For example, the base-drag model of Tadakuma et al. over-predicts the base-drag contribution for a heavy-truck platoon by more than 50%. The relationship between wake-effect drag reduction and the net drag of preceding vehicles therefore leads to cumulative errors in the subsequent sub models, limiting the usefulness of direct comparisons.

The model of Schmid et al. [7] may prove more useful as a starting point, due to their truck-specific definitions. However the insufficient description of units and normalizations to define the empirical constants in their paper limited the ability to adopt their truck-specific formulations, and to perform comparisons, in the development of this new model. The following sections describe the various sub models with some reference to the models of Tadakuma et al. and Schmid et al., but without direct comparisons.

Base-Drag-Reduction Model

As the separation distance is reduced, the field of high-pressure at the front of the trailing vehicle increases the base pressure of the lead vehicle, effectively giving it a push and reducing its drag. Tadakuma et al. [6] introduced an empirically-tuned model based on an analytical expression from a potential-flow solution. Their model, which defines the change in drag coefficient relative to the isolated-vehicle drag, is a function of separation distance, X_S, and a single empirical constant. Schmid et al. [7], whose model is specific to truck platooning, noted that two empirical constants were required to provide a reliable prediction. Their source data, however, are inferred drag reductions based on conversion of fuel-savings data (from this author's work [13]), not from measured drag reductions.

The base-drag-reduction model was developed by first characterizing the effect without cross winds, using a formulation similar to Tadakuma et al. [6] and Schmid et al. [7], with adaptations to fit better the source data from the 1/15-scale wind-tunnel tests. The change in drag coefficient for Truck n at 0° yaw angle is modelled as:

$$\Delta C_{D0base,n} = -\left(1-\left(1-\left(\frac{8.5\text{ m}}{X_S+19\text{m}}\right)^3\right)^2\right)*\cdots \\ max\left[\left(1-\frac{X_S}{25\text{m}}\right),0\right]\frac{\left(C_{D0,n}/C_{D0ref,n}\right)}{\left(C_{D0,n-1}/C_{D0ref,n-1}\right)}SF_{base} \quad (2)$$

This model is shown, with the corresponding wind-tunnel data for four trailer configurations, in Figure 1. The first term with nested brackets is analogous to the other models, with the constants (8.5 m and 19 m values) tuned from the wind tunnel data. The "max" term of Equation 2 is necessary to damp the influence at larger distances, to prevent drag reductions for separation distances beyond 25 m, beyond which most aerodynamic and fuel-economy results have shown no influence to the base drag. Here, the C_{D0}/C_{D0ref} terms introduce a level of proportionality to the isolated-vehicle C_D value for conditions in which the truck is not the first within the platoon. It ties the effect directly to the wake-effect model defined in the next section (Equation 10), with the ratio of the terms representing a relative strength that accounts for the lower-wind-speed environment of upstream trucks, and only affects platoons with three trucks or more. For Truck n = 1, this wake-term ratio is set to 1. Equation 2 is only applied to trucks 1 to N – 1 of an N-truck platoon because the last truck does not experience a base-drag reduction.

The final term in Equation 2, SF_{base}, is a scaling factor used to adjust the base-drag-reduction effect for different trailing-tractor types. This factor was added upon

FIGURE 1 Base-drag-reduction data at 0° yaw angle for the 1/15-scale wind-tunnel data and the model of Equation 2.

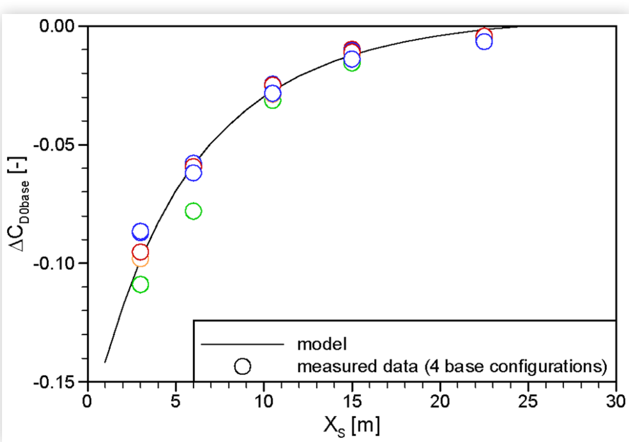

FIGURE 2 Sample base-drag-reduction corrections for yaw-angles up to ±15° and lateral-offset of 0 and 0.8 m, using Equation 3.

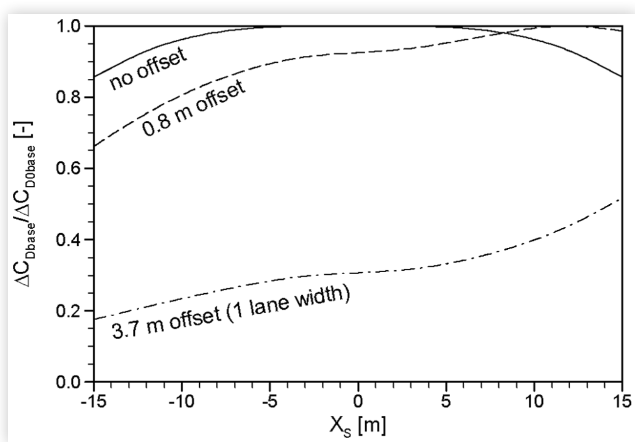

comparison of the cab-over-truck data of Törnell et al. [2]. SF_{base} = 1 for long-nose tractors and SF_{base} = 1.7 for cab-over tractors.

The base-drag-reduction effect shows small sensitivity to yaw angle for an aligned platoon, with some reduction in its magnitude for yaw angles exceeding ±10°. However, when lateral offsets between trucks are introduced, the peak base-drag reduction is observed at a shifted yaw angle representing a condition where the trailing truck is offset towards the wind-ward direction. It may be possible to develop a cross-wind and lateral-offset correction model based on a potential-flow solution, like the approach of Tadakuma et al. [6] for aligned platoons, but the magnitudes of the changes are small relative to overall drag reductions of the truck-platoon system and therefore such an approach is not necessary here. As such, an empirical correction has been developed that accounts for yaw-angle, ψ, and lateral offset, Y_{off}, effects using a single hyperbolic secant function:

$$\frac{\Delta C_{Dbase}}{\Delta C_{D0base}} = sech\left(0.005\psi\,\left|\psi\right|^{0.75} + 0.5Y_{off}\right) \tag{3}$$

where ψ, is in degrees, and Y_{off} is in m. This model represents the general trends observed in the 1/15-scale wind-tunnel data set, including a full-lane offset condition for which the effect is present but at much-reduced magnitude. Figure 2 shows Equation 3 for aligned and two offset conditions, representing a large within-lane offset (0.8 m) and a full-lane-width offset (3.7 m).

Flat-bed-trailer data from the track-test source data [14] show a reduced magnitude of the base-drag effect when the flat-bed is in the forward position, because the size of the surface over which the increased pressure can act is reduced. Therefore, a first approximation to correct Equation 2 for lower-height trailers, that replicates the trends observed in the flat-bed fuel-savings data, is to scale its magnitude by the ratio of the base area to that of a standard box-van trailer ($A_{base,DV}$=10.7 m^2).

The final form used for the base-drag effect is:

$$\Delta C_{Dbase,n} = \Delta C_{D0base,n}\left(\frac{\Delta C_{Dbase}}{\Delta C_{D0base}}\right)\left(\frac{A_{base}}{A_{base,DV}}\right) \tag{4}$$

for which the first two terms are defined by Equations 2 and 3 and the last being the area scaling term for lower-height trailers. Validation of this model is demonstrated in a later section of this paper.

Wake-Effect Drag-Reduction Model

The wake-effect model is based predominantly on the physics of wake-decay processes downstream of bluff-bodies in close proximity to the ground. The models of Tadakuma et al. [6] and Schmid et al. [7] are both based on the classic power-law decay model for an axisymmetric wake, with a -2/3 decay exponent. In the 1/15-scale wind-tunnel wake-survey experiments of the author [18], the power-law exponents associated with the peak-deficit decay and the spatial-spreading match better the values derived by Eskridge and Thompson [20] specific to wakes adjacent to a ground plane. Therefore, the Eskridge and Thompson model, with a -3/4 decay exponent, has been adapted for the current model, with changes to the empirical constants to reflect the greater fidelity of the wake-flow measurements available. The wind-speed-deficit decay model used here, specific to the wake of Truck n, is defined by:

$$\frac{U_{\min,n}}{U_{ref}} = 1 - \Lambda C_{D0,n}^{1/4}\left(\frac{X_S}{H}\right)^{-3/4} \tag{5}$$

where a value of 0.65 has been defined for Λ based on the 1/15-scale wind-tunnel aerodynamic-drag data for which wind-speed measurements were made forward of the aft-truck grille [1], and based on the 2019 track-test data for which wake measurements were examined in detail [15]. These data and the model of Equation 5 are shown in Figure 3. Assuming that the trailing truck will experience a uniform reduction of wind speed according to Equation 5, a wake-deficit (wd) drag-reduction effect can be defined for a trailing vehicle as:

$$\frac{C_{D0wd,n}}{C_{D0ref,n}} = \left[1 - \Lambda C_{D0,n-1}^{1/4}\left(\frac{X_S}{H}\right)^{-3/4}\right]^2 \tag{6}$$

Due to various factors, including the spatial extent of the wake, its shape, and the interaction of the wake-deficit distribution over the drag-producing surfaces of the trailing truck, Equation 6 over-predicts the magnitude of drag reduction. The models of Tadakuma et al. [6] and Schmid et al. [7] formulate the correction for this effect in different ways, and here a different approach is also taken. Using 2-truck aerodynamic-drag data from the 1/15-scale wind-tunnel tests and the 2019 track tests, and approaching the correction formula in a similar power-law manner to the wake-deficit formula, the following

FIGURE 3 Wake-wind-speed decay measurements and model of Equation 5.

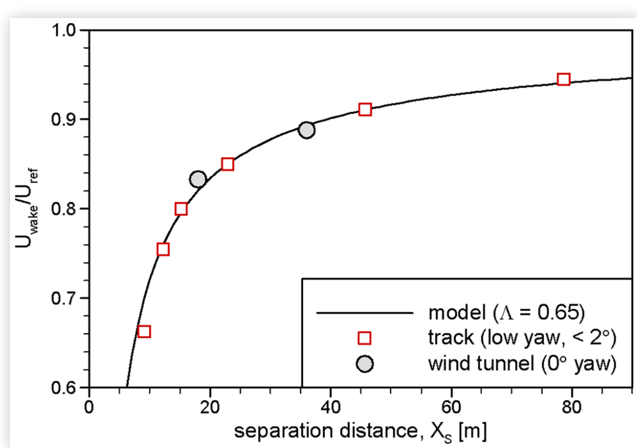

© National Research Council Canada

relationship was found to apply well for what is here named the wake-shape correction:

$$\frac{C_{D0,n}}{C_{D0wd,n}} = \left[1 + BC_{D0ref,n-1}^{1/2}\left(\frac{X_S - X_{Soff}}{H}\right)^{-3/2}\right] \tag{7}$$

where the empirical constants B and X_{Soff} depend on the truck configuration. The first formulation of this wake-shape-correction term only contained the B parameter, but when investigating this model's use for cab-over truck configurations, an offset to the separation distance (X_{Soff}) was needed to ensure reliable predictions. Figure 4 shows this relationship which highlights the differentiation between flat-base and boat-tail configurations, and the difference with the cab-over tractor shapes. The cab-over data are based on data from Törnell et al. [2]. The long-nose-truck data show two distinct bins of results defined by the two B values of 3.2 and 3.7 in Figure 4, consistent with whether the trailer has a boat-tail or not. The value of 3.2 is consistent between the track test data (skirts+tail-outfitted trailer) and the 1/15-scale wind-tunnel data with boat-tails. Furthermore, these two values replicate the short-separation-distance trends of the 1/50-scale wind-tunnel data for truck types with and without a boat-tail (not shown explicitly here). The cab-over values (B = 3.0 with X_{Soff} = 1.3 m) are based on a single high-fidelity-CFD data set, and may require additional experimental validation.

Combining Equations 6 and 7 provides the ratio of the 0°-yaw-angle drag-coefficient relative to the reference isolated condition:

$$\frac{C_{D0,n}}{C_{D0ref,n}} = \left[1 + BC_{D0ref,n-1}^{1/2}\left(\frac{X_S - X_{Soff}}{H}\right)^{-3/2}\right] * \cdots \left[1 - \Lambda C_{D0,n-1}^{1/4}\left(\frac{X_S}{H}\right)^{-3/4}\right]^2 \tag{8}$$

FIGURE 4 Wake-shape-constant definition based on formulation of Equation 7.

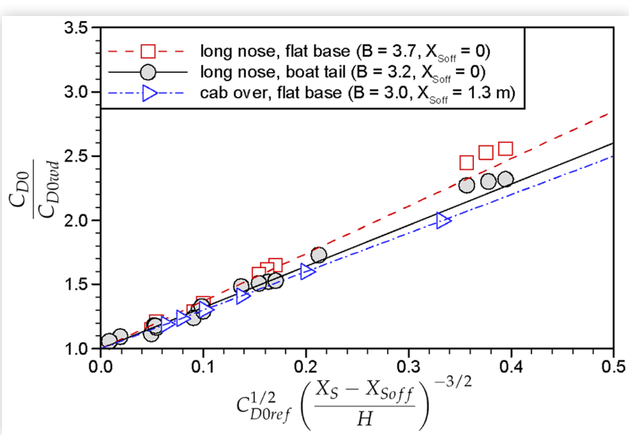

© National Research Council Canada

As will be shown later, this formulation predicts reliably the non-linearities of the close-proximity platooning effect. Wind-tunnel and track studies generally show an increase in drag-reduction (or corresponding fuel-savings) as the separation distance is reduced from large distances down to about 15 m to 20 m. At closer distances, the trend reverses and the benefit decreases with decreased separation. This drag-reduction reversal is replicated by Equation 8, and this agreement is associated with the wake-shape correction term B.

The flat-bed-trailer scenario tested on the track suggests that Equation 8 requires adjustment for non-van trailers. The fuel-savings data from the track tests [14] show that, unlike the flatbed-configured lead truck that experienced a reduced benefit due to its smaller base area, the following truck does not exhibit the reduced benefit in the sub-15 m range discussed in the last paragraph. A modification is required to account for the different wake-development processes that occur with a base height that does not match either the following-vehicle height or the maximum height of the source vehicle itself. The first of these effects, for different overall vehicle heights, is expected to be addressed through an adjustment to the B parameter for this different mixed-combination of truck configurations, while the second effect requires some additional insight into the source of the wake.

For a high-roof tractor paired with a flat-bed trailer, the size and shape of the wake will be somewhat similar to that for the dry-van trailer but with an effective source location for the upper part of the wake at the base of the tractor, not at the base of the trailer. To account for this, a simple adjustment has been introduced to each of the two wake-effect terms of Equation 8. For the wake-deficit term, the "separation distance" is extended to represent an area-averaged weighting of the distance from the nose of the trailing truck to the base of the leading truck and of the distance to the tractor base (or other large body on the flatbed). For the wake-shape term, the full extended distance (to the base of the lead tractor or large body on the flat-bed) is used since this distance likely determines the wake structure that interacts with the following vehicle. Introducing the base-area ratio ($AR_{base} = A_{base}/A_{ref}$) and the extended distance from the base to the tallest surface (X_{ext}), Equation 8 is updated to the following form:

$$\frac{C_{D0,n}}{C_{D0ref,n}} = \left[1 + BC_{D0ref,n-1}^{1/2}\left(\frac{X_S - X_{Soff} + X_{ext}}{H}\right)^{-3/2}\right] * \cdots \left[1 - \Lambda C_{D0,n-1}^{1/4}\left(\frac{X_S + X_{ext}\left(1 - AR_{base}\right)}{H}\right)^{-3/4}\right]^2 \tag{9}$$

This version of the wake-drag-reduction equation demonstrates the correct changes to the fuel-savings trends exhibited with a flat-bed trailer in the lead position of a platoon.

For platoons longer than two vehicles, a trailing vehicle experiences drag reduction not just from its predecessor in the line of vehicles but from all upstream vehicles. When applying the wake-effect model of Equation 9, these compounded wake effects must be included. For the purpose of the current model, an assumption has been made that all upstream vehicles contribute to the peak drag reduction at zero yaw angle through an adaptation of this equation. To account for all upstream vehicles Equation 9 has been modified in the following manner:

$$\frac{C_{D0,n}}{C_{D0ref,n}} = \prod_{i=1}^{n-1} \left[1 + B_i C_{D0ref,i}^{1/2} \left(\frac{X_{SeffB,i}}{H_i} \right)^{-3/2} \right] * \cdots \left[1 - \Lambda C_{D0,i}^{1/4} \left(\frac{X_{SeffA,i}}{H_i} \right)^{-3/2} \right]^2 \quad (10)$$

where the effective separation distances for each term, X_{SeffA} and X_{SeffB}, are based on the distance from the vehicle of interest (n) to the effective source location of the wake for the respective upstream vehicle (i) and defined as:

$$X_{SeffB,i} = \left(\sum_{j=2}^{i} L_j \right) + \left(\sum_{j=1}^{i} X_{S,j} \right) - X_{Soff,i} + X_{ext,i} \quad (11)$$

and

$$X_{SeffA,i} = \left(\sum_{j=2}^{i} L_j \right) + \left(\sum_{j=1}^{i} X_{S,j} \right) + X_{ext,i} \left(1 - AR_{base,i} \right) \quad (12)$$

where L_j is the length of vehicle j.

Cross-Wind and Lateral-Offset Model

Equation 10 represents strictly the drag reduction from wake effects for an aligned platoon without cross winds. To include the effect of cross winds, by means of the yaw angle of the wind, consideration must be given to the shape and trajectory characteristics of the wake. In [18], the author shows a complex wake structure downstream of HDVs with cross winds. The wake consists of a large vortex-wake structure, with the vortex emanating from the windward top edge of the trailer roof. Depending on the truck configuration, multiple wake cores (local deficit maxima) may be present, with one near the ground and one near the centre of the vortex. As the yaw angle increases, the top part of the wake convects in the direction of the cross wind to a greater extent than the low part of the wake, creating a wide sheared wake. To simplify the wake definition for the current model, the wake characteristics at mid-truck-height are considered to be an appropriate metric. Following the model of Eskridge and Thompson [20], but only considering the lateral coordinate, y, the shape of a wake can be defined in the following manner:

$$\frac{U_n(y)}{U_{ref}} = 1 - \Lambda C_{D0,n}^{1/4} \left(\frac{X_S}{H} \right)^{-3/4} e^{-\eta^2/8} \quad (13)$$

where

$$\eta = y \left[\gamma H \Lambda C_{D0}^{1/4} \left(\frac{X_S}{H} \right)^{\alpha} \right]^{-1} \quad (14)$$

The term in the square bracket of Equation 14 is a characteristic-width parameter for which the values of the wake-width constant, γ, and the wake-spreading-rate constant, α, have been selected based on a best visual fit of the mid-height wake profiles from the 1/15-scale wind-tunnel wake-survey experiments. The wake-spreading-rate value of $\alpha = 0.25$, defined by Eskridge and Thompson [20], is retained and is consistent with the wake-spreading-rate results of [18]. A wake-width-constant value of $\gamma = 0.14$ provides a modelled wake width similar to the experimentally-measured wakes. These values appear to apply equally to the different trailer configurations with a long-nose tractor, but have not yet been validated for cab-over configurations.

With cross winds, the centre of the wake (location of peak wind-speed deficit) shifts laterally towards the leeward side and therefore a trailing vehicle does not necessarily experience the same magnitude of predicted zero-yaw wind-speed deficit. At large separation distances and large yaw angles, or large lateral offsets, the trailing truck may reside completely outside of the wake region. Therefore, consideration must be given for the lateral shift in the wake, and a simple model has been introduced to scale appropriately the drag-reduction magnitude from Equation 8. To model the wake shift, a simple algebraic relation is introduced for each principal wake type (with or without a boat-tail), defined from the 1/15-scale wind-tunnel wake-survey measurements and based on the normalized lateral wake coordinate (η, Equation 14) modified accordingly:

$$\eta = \left(y + R_{WO}(\psi) X_S + Y_{off} \right) \left[\gamma H \Lambda C_{D0}^{1/4} \left(\frac{X_S}{H} \right)^{\alpha} \right]^{-1} \quad (15)$$

where Y_{off} is the lateral offset between the trucks and R_{WO} is a wake-offset-ratio parameter that relates the lateral position of the wake centre to the separation distance. This parameter is found to be a function of yaw angle and trailer type, as shown in Figure 5. These data were measured 14 base-widths downstream of the truck models, and match well data measured at 7 base-widths, suggesting that the trend is represented for a significant distance downstream of a truck. For a conventional flat-base trailer, the wake-offset-ratio parameter is defined as:

$$R_{WO}(\psi) = \begin{cases} 0.000416\psi^2 + 0.00546\psi, & \text{for } \psi >= 0^\circ \\ -0.000416\psi^2 + 0.00546\psi, & \text{for } \psi < 0^\circ \end{cases} \quad (16)$$

FIGURE 5 Wake-offset-ratio measurements from 1/15-scale wind-tunnel wake-survey measurements and models of Equations 16 and 17.

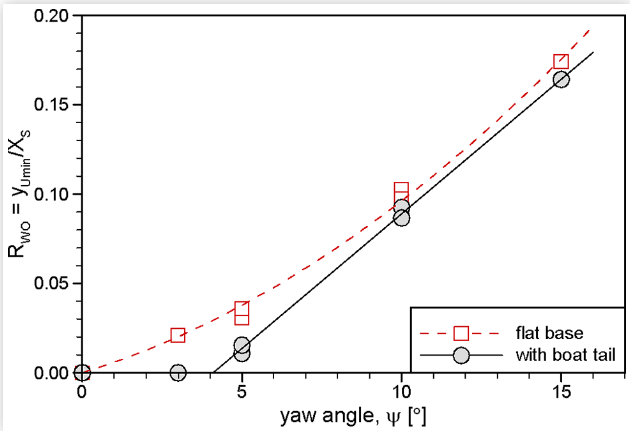

© National Research Council Canada

For a boat-tail-outfitted trailer, the wake-offset-ratio parameter is defined as:

$$R_{WO}(\psi) = \begin{cases} 0.0151\psi + 0.0621, & \text{for } \psi < -4.1^\circ \\ 0, & \text{for } \psi >= -4.1^\circ \text{ and } \psi <= 4.1^\circ \\ 0.0151\psi - 0.0621, & \text{for } \psi > +4.1^\circ \end{cases} \quad (17)$$

These wake-offset-ratio definitions show that the wake centre does not shift laterally to the same extent that would be predicted by direct convection with the freestream winds. This is also consistent with side-wash observations in road-vehicle-wake flows [18]. In particular, the boat-tail-equipped-trailer model shows that the wake centre remains aligned with the truck centre line for any yaw angle within about 0±4°.

When validating the yaw-angle and lateral-offset contributions of the model, three additional considerations were included in the model.

First, it was recognized that the wake-width grows not just with longitudinal distance, but with yaw angle as well, as exemplified in the results of [18]. To account for this, a simple linear-growth-with-yaw parameter was added with a rate of 7% per degree.

Secondly, the source data suggest that using a distance greater than X_S in Equation 15 improves the influence of the lateral shift in the wake associated with the wake-offset-ratio parameter and the lateral spreading rate. Adding half the truck length (0.5*L*) provides an improvement in the results, particularly at shorter separation distances. This represents moving the wake source to the middle of the truck, rather than its base.

Thirdly, at small separation distances and large lateral offsets, the results suggested that the wake-offset-ratio parameter should be larger. For these conditions, a direct projection from the truck centre based on the freestream (*fs*) wind direction improved the prediction:

$$R_{WO,fs} = \tan(\psi) \quad (18)$$

Lateral-offset data up to one lane width (3.7 m) was available from two data sets, including the 1/15-scale wind-tunnel results [1] and the 30%-scale wake-effects results using a wake-generator system [19]. Based on these results, a combination of the two R_{WO} options are used with the proportionality of each depending on X_S and Y_{off}, as follows. Assuming that Equations 16 or 17, which were defined based on flow measurements, are represented as $R_{WO,meas}$, then the following linear proportionalities are applied:

$$R_{WO,near} = \begin{cases} \left(1 - \frac{|Y_{off}|}{3.7\text{ m}}\right) R_{WO,meas} + \left(\frac{|Y_{off}|}{3.7\text{ m}}\right) R_{WO,fs}, & \text{for } |Y_{off}| < 3.7\text{ m} \\ R_{WO,fs}, & \text{for } |Y_{off}| \geq 3.7\text{ m} \end{cases} \quad (19)$$

representing a ration for near-wake conditions, and

$$R_{WO} = \begin{cases} \left(1 - \frac{|X_S|}{50\text{ m}}\right) R_{WO,near} + \left(\frac{|X_S|}{50\text{ m}}\right) R_{WO,fs}, & \text{for } X_S < 50\text{ m} \\ R_{WO,meas}, & \text{for } X_S \geq 50\text{ m} \end{cases} \quad (20)$$

To evaluate the drag reduction of a following truck with cross winds and/or with lateral offset between the vehicles, the 0°-yaw-angle drag-reduction (defined by Equation 10) is scaled using the ratio of the wind-speed deficit at $y = 0$ (ΔU along the lead-truck centreline) to the value predicted at the wake centreline (ΔU_0):

$$\frac{C_{D,n}}{C_{Dref,n}} = 1 - \left(1 - \frac{C_{D0,n}}{C_{D0ref,n}}\right)\left(\frac{\Delta U}{\Delta U_0}\right)^2 + \frac{\Delta C_{Dbase,n}}{C_{D0ref,n}} \quad (21)$$

where the ΔC_{Dbase} term is that defined by Equation 4 which already accounts for yaw angle and lateral offset. Equation 21 is the square-bracket drag-reduction-ratio term of Equation 1. Its formulation, with the wind-speed-deficit ratio squared, is a linearized form of the fully-expanded equation, with the linearization having a negligible influence on the final result. The wind-speed-deficit ratio, accounting for the trajectory of the wake and for a specified lateral offset, is defined as:

$$\left(\frac{\Delta U}{\Delta U_0}\right) = e^{-\frac{1}{8}\left(R_{WO}(\psi)\left(X_S + \frac{1}{2}L\right) + Y_{off}\right)^2 * \ldots} \left[\gamma \Lambda C_{D0}^{1/4} \left(\frac{X_S + \frac{1}{2}L}{H}\right)^{\alpha} \left(1 + 0.07\,|\psi|\right)\right]^{-2} \quad (22)$$

Combining Equation 21 with Equations 4, 10 and 22, the ratio of the drag coefficient of a trailing vehicle to its corresponding isolated condition at the same yaw angle is calculated. The next section will define the final step necessary towards calculating the drag-coefficient of a truck in platoon formation.

The no-cross-wind wake-effect term in Equation 21 ($C_{D0,n}/C_{D0ref,n}$) is formulated to account for all upstream vehicles, per its form in Equation 10. Although the wake flow-field experienced by a truck will be influenced by all preceding trucks, the model of Equation 22 assumes that the yaw and lateral-offset effects are only influenced by the immediate predecessor vehicle. This assumption effectively states that the wake-shape characteristics that affect the drag reduction with cross winds or with laterally-offset vehicles are strictly a function of the preceding vehicle and that the further-forward vehicles contribute only to the overall decrease in the effective wind speed.

Effective Yaw-Angle Model

The model thus far predicts the correct trends for the drag-coefficient as a function of separation distance, lateral offset and yaw angle, but somewhat under predicts the magnitude of the drag reduction (over predicts the drag coefficient) at yaw conditions. A trend that is not replicated well by this model is the flattening of the $C_D(\psi)$ curve in the ±5° range that has been observed in the track-test aerodynamic results [15] and the 1/15-scale wind-tunnel results (not explicitly shown but subsequently observed in the results of [1]). In the aerodynamic analysis of the track-test measurements, McAuliffe et al. [15] documented the side wash in the wake that acts to reduce the effective yaw angle experienced by the trailing vehicle, while in some cases reversing the flow directionality relative to the freestream. Those results are reproduced here as the symbol data in Figure 6. This behaviour has been attributed to a large vortex that is generated at yaw conditions, with the wake-survey wind-tunnel data (measured at mid truck height) showing similar side-wash magnitudes and trends to the track data.

This vortex-induced side-wash phenomenon suggests that the reference C_{Dref} value in Equation 21, which was defined to correspond to the reference drag-coefficient performance at the freestream yaw angle (C_{Dref} (ψ_{fs})), should instead be evaluated at the effective yaw angle resulting from the change in wake-flow angularity (C_{Dref} (ψ_{eff})). Initial checks using the experimental data have demonstrated that this approach adjusts the drag reduction to an appropriate magnitude and flattens the $C_D(\psi)$ curve in an appropriate manner. The only constraint required to limit strange behaviour of the model is to limit complete reversal of the flow angularity such that the largest possible reduction in yaw angle reduces the effective yaw angle to 0°.

An "effective yaw angle" model has been developed based on yaw-angle measurements observed from the track-test data (data from Figure 6), the 1/15-scale wake-survey-data, and the 1/15-scale aerodynamic-drag study that included flow measurements forward of the front grille of the aft truck model. An analytical expression has been developed that introduces an appropriate change in magnitude of the effective yaw angle based on separation distance and lateral offset. The change in effective yaw angle is defined as:

FIGURE 6 Effective yaw angle in the wake of a truck. Symbols are experimental data from track measurements [15]. Lines represent the model of Equation 23.

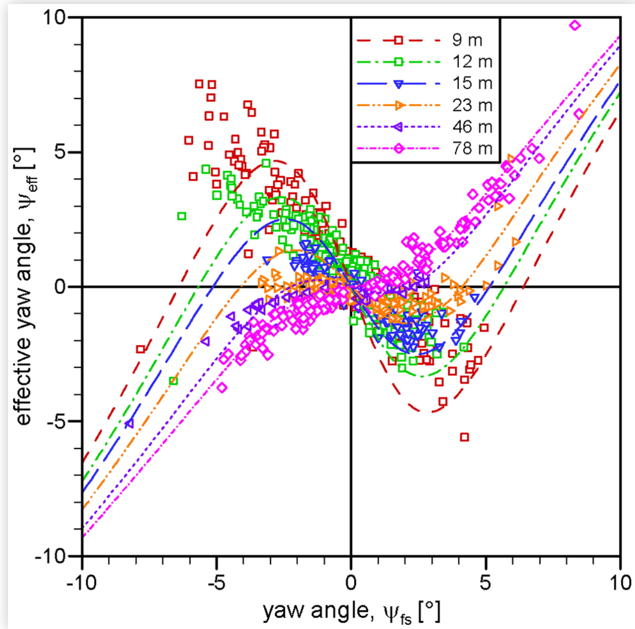

© National Research Council Canada

$$\Delta\psi_{eff} = 3.34 SF_{\psi}\left(\frac{X_S}{H}\right)^{-0.76}\tanh\left(0.315\left(\frac{X_S}{H}\right)^{0.11}\psi_{fs}\right)*\cdots$$
$$\operatorname{sech}\left(0.2\left[\psi_{fs}+\operatorname{atan}\left(\frac{Y_{off}}{X_S}\right)\right]\right)\left(\frac{\Delta U}{\Delta U_0}\right)^{0.1} \quad (23)$$

which is shown, when subtracted from the freestream yaw angle, to match well the track measurements in Figure 6. The effective yaw angle is then defined as:

$$\psi_{eff} = \begin{cases}\psi_{fs} - \Delta\psi_{eff}, & \text{for } |\psi_{eff}| < |\psi_{fs}| \\ 0, & \text{for } |\psi_{eff}| > |\psi_{fs}|\end{cases} \quad (24)$$

In Equation 23, the SF_{ψ} parameter adjusts the strength based on the trailer configuration, such that SF_{ψ} = 1.0 if side skirts are installed, otherwise SF_{ψ} = 0.5. The first power-law term (with exponent -0.76) controls the magnitude of the effects of separation distance. The hyperbolic-tangent function controls the anti-symmetric nature at positive and negative yaw along with the slope of the yaw-angle correction about 0° free-stream yaw. The hyperbolic-secant function controls the decay of the correction with increasing yaw angle and shifts the weighting of the function when the trucks are offset laterally. The wake wind-speed-deficit ratio to the power of 0.1 limits the extent of the effective yaw angle if the trailing truck resides outside of the wake region. With the effective yaw angle from Equations 23 and 24, the-isolated vehicle reference drag coefficient is then calculated or interpolated from the C_{Dref} (ψ) definition, and used in Equation 1 to calculate the drag coefficient of the platooning truck.

Validation The model formulation in Equation 1 and its sub models were developed based on examination and subsequent validation against the various data sets available for various separation distances, yaw angles, and lateral offsets. Demonstration of the model validity, via comparison of its predictions of drag performance to four data sets, is demonstrated in the following.

1/15-scaleWind-Tunnel Aerodynamics-Drag Experiments

The aerodynamic performance of a two-truck platoon was measured by McAuliffe and Ahmadi-Baloutaki [1]. These data were used primarily to develop the model and tune its empirical coefficients. The comparisons in this section are therefore verifications of the implementation, rather than a true validation. Subsequent sections provide some direct validations.

Drag-coefficient results are shown in Figures 7 and 8 for a two-truck platoon of long-nose North-American-style tractors paired with two different box-van-trailer configurations, based on acquired data over a yaw-angle range of ±15° [1]. In the figures, each row represents a different separation distance, X_S, which is not necessarily coincident amongst the two figures. The left column shows data for a basic trailer, while the middle and right columns show data for an aerodynamic trailer with side skirts and a boat tail. The left and middle columns represent aligned trucks, with the right column showing data for a lateral offset of -0.8 m (which represents the aft truck shielded to a greater extent at positive yaw angles). Each plot shows the C_D values of the isolated-truck and the corresponding trailing truck of the two-truck platoon, with the difference (ΔC_D) represented using a different scale to emphasize the differences.

For the lead truck, in Figure 7, the experimental data show that drag reduction is predominantly a function of separation distance, with minimal influence of yaw angle and lateral offset. At the smallest separation distance of 6 m (top row), some differences between the model and experimental data are observed at higher yaw angles, but the general magnitudes and trends are represented well. At the larger separation distance of 15 m, the differences between the model and experimental data are within the experimental uncertainty (height of the symbols) for all except the +15°-yaw-angle condition.

FIGURE 7 Model predictions compared to sample 1/15-scale experimental wind-tunnel measurements for the lead truck of a two-truck platoon configuration at different separation distances, X_S, lateral offsets, Y_{off}, and yaw angles, psi_{fs} (Trailer N - with "N"o aerodynamic devices, Trailer C - with "C"ombined configuration of side skirts and boat tails). Symbol size is the approximate magnitude of the measurement uncertainty of the dependent parameter.

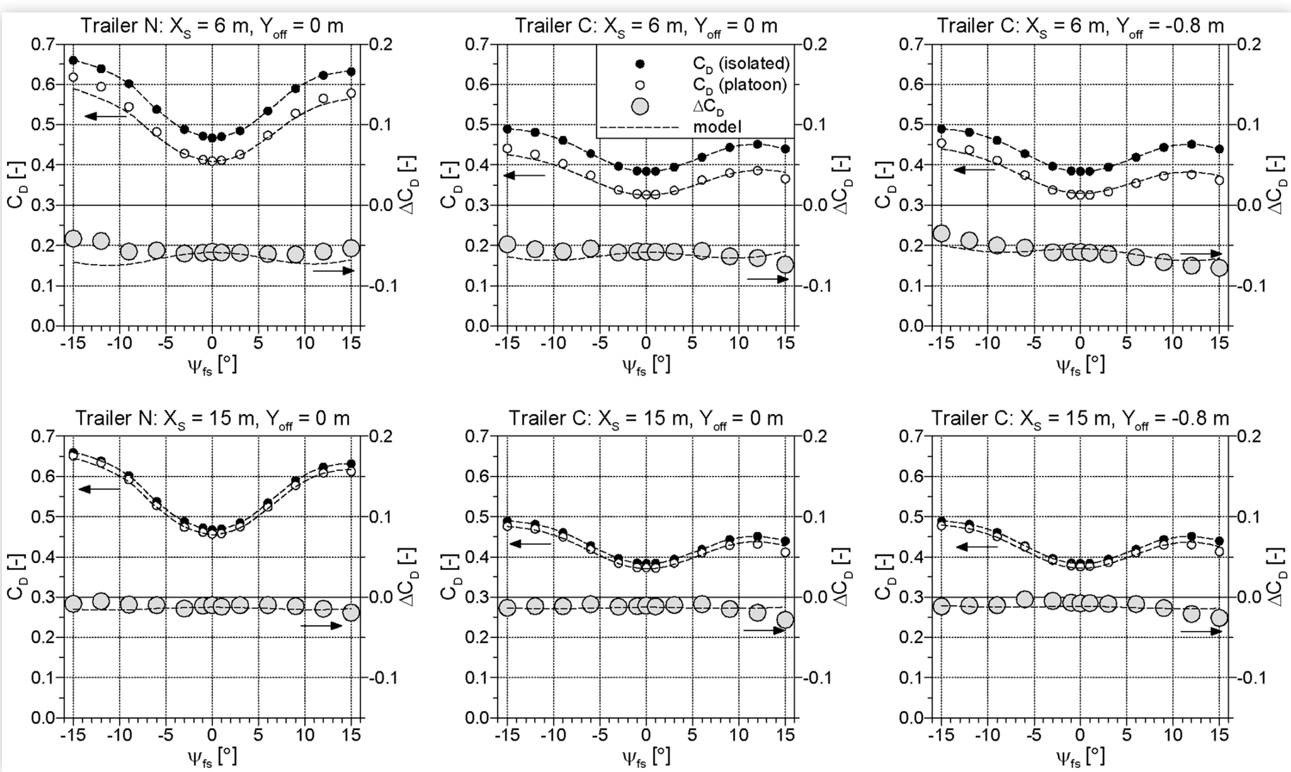

© National Research Council Canada

FIGURE 8 Model predictions compared to sample 1/15-scale experimental wind-tunnel measurements for the trailing truck in a two-truck platoon configuration at different separation distances, X_S, lateral offsets, Y_{off}, and yaw angles, psi_{fs} (Trailer N - with "N"o aerodynamic devices, Trailer C - with "C"ombined configuration of side skirts and boat tails). Symbol size is the approximate magnitude of the measurement uncertainty of the dependent parameter.

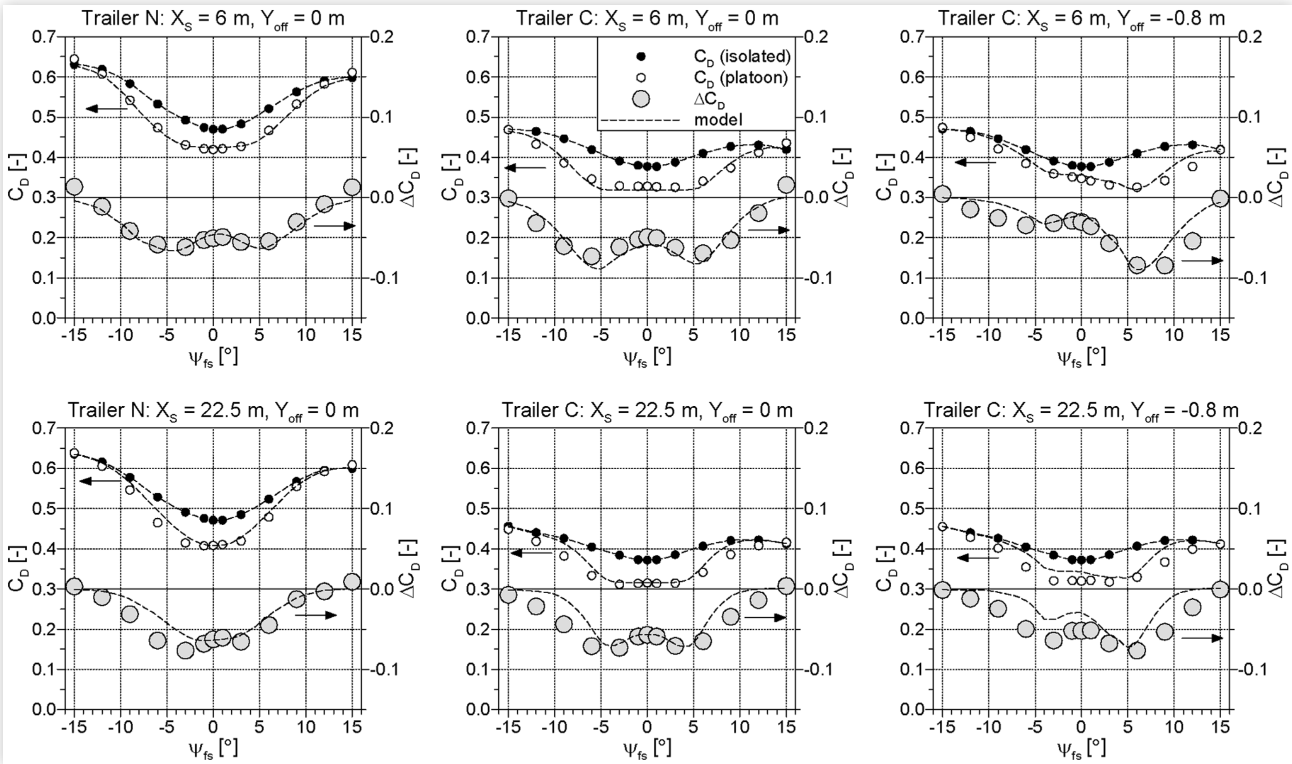

© National Research Council Canada

For the trailing truck in Figure 8, all the zero-offset platoon data show a flattening of the $C_D(\psi_{fs})$ curves at low yaw-angle magnitudes, which results in double-peak ΔC_D characteristic. This double-peak ΔC_D is a combined result of the wake-shielding effect maintained to a higher yaw angle, and a reduced effective yaw angle. This combination has the greatest influence at moderate yaw angles around ±5° at these smaller separation distances. Laterally offsetting the trailing truck amplifies this influence when the trailing truck is shielded from the freestream wind to a greater extent (+ yaw angles here). Evident in these figures is the ability of the model to adequately capture the trends associated with these phenomena, and the associated magnitudes. Conditions with larger lateral offsets and higher yaw-angle magnitudes show an under prediction of the drag-reduction benefit. This difference may be attributed to limitations with the wind-tunnel experiments. McAuliffe et al. [17] highlight, for experiments using fixed-floor wind-tunnel arrangements, that vehicle models interact with the floor boundary layer, creating horseshoe-vortex structures that effectively widen the wakes. Wider wakes would over-emphasize the platooning benefit at larger yaw angles and at larger later offsets, and it is unclear whether these discrepancies are due to deficiencies of the prediction model or the experiments. However, these higher-yaw or larger-offset conditions occur less often and will have a smaller influence on predictions of long-term benefits.

Track Aerodynamic Drag Experiments

Real-world aerodynamic performance of a two truck platoon is shown in Figure 9, based on a constant-speed driveshaft-torque-based test methodology [15], providing validation data at large separation distances (9 m to 78 m). Only trailing-truck data are shown here for validation purposes, due to excessive measurement uncertainty for the lead-vehicle. The trailing-truck data include large-distance wake influences that are experienced by trucks at everyday safe-distance driving conditions. Although cross winds were not excessive during the experiments, data up to yaw angles of about ±5° were captured. The left plot of Figure 9 shows the variation with yaw angle of C_D for the isolated truck and for two trailing-truck scenarios of 9 m and 46 m separation distance, relative to the zero-yaw C_D value of the isolated truck. The black and grey lines represent the experimentally-determined C_D characteristics with their 95%-confidence uncertainty bounds. The coloured lines show the predictions from the model, demonstrating good agreement of drag-reduction trends and magnitudes with the experimental data. The flattened C_D curve is again apparent here, with the drag beginning to increase around 4° to 5° yaw angle.

The right plot of Figure 9 shows, for two yaw angles, the variation in drag-reduction with separation distance, which highlights two particular phenomena observed in

FIGURE 9 Model predictions compared to sample experimental track measurements for a two-truck platoon configuration at different separation distances and yaw angles. Grey lines in left plot represent 95% confidence levels of corresponding experimental data.

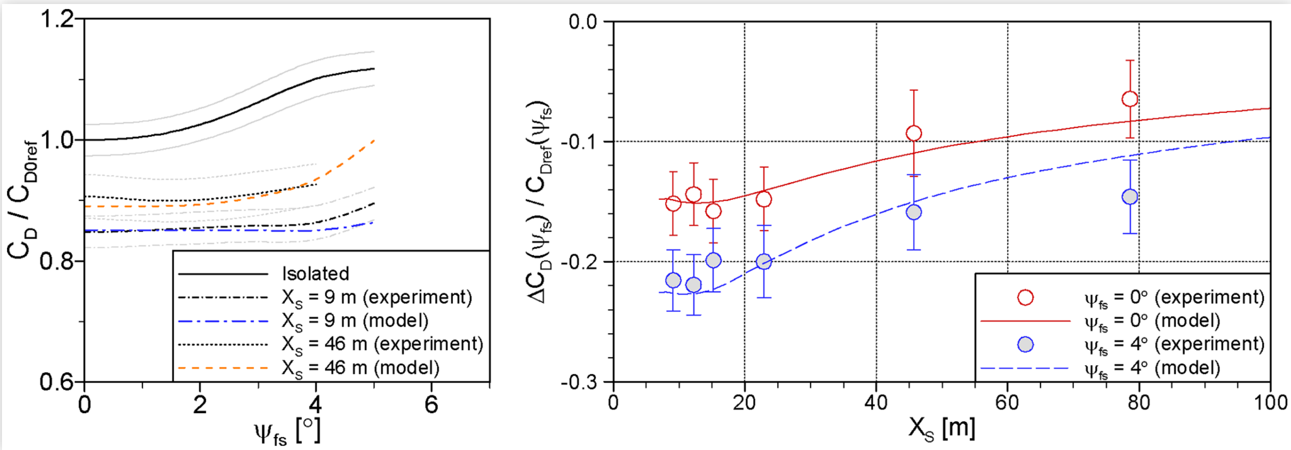

© National Research Council Canada

various studies. Beyond about 15-20 m separation distance, the drag-reduction benefit reduces with increasing separation distance due to decay of the wake. As separation distance reduces below about 15 m, these and other data sets [1, 8, 9] show a reduced sensitivity to distance, often with a decreasing benefit, which is captured by the model. For the range of separation distances of the track-test data (9 to 78 m), the model provides a reasonably good prediction of the trends and magnitude. Only at the largest distance (78 m) and the highest yaw angle (4°) does the model fall outside the uncertainty bounds of the experimental data. Despite this, the model is shown to be valid for a large range of truck-separation conditions.

1/50-scaleWind-Tunnel Aerodynamics-Drag Experiments

The 1/50-scale wind-tunnel results of Salari and Ortega [8] include data for a three-truck platoon. For consistency with their presentation of results, platoon drag reduction was first calculated at various yaw angles (over a range of ±9°) and subsequently used to calculate a wind-averaged drag coefficient (WAC_D, per the SAE J1252 method [22]) at each truck-spacing condition.

Figure 10 shows the experimental results and predictions for a platoon of three trucks with long-nose tractors and skirts-outfitted dry-van trailers. Data are normalized to the wind-averaged drag coefficient of the isolated truck, with results for each of the three trucks in the left plot, and the platoon average in the right plot. The platoon configuration has a 15 m separation (full scale) between the lead and middle trucks, with variable separation between the middle and trailer trucks as represented by the abscissa in the plots. The model predictions for the lead and middle trucks are reasonably good and fall within the experimental uncertainty, or close to it, for most of the separation distances. The prediction for the trailing truck shows the same general trend as the experimental data but with an

FIGURE 10 Model predictions of the wind-averaged-drag coefficient for a three-truck platoon compared to sample 1/50-scale experimental wind-tunnel measurements of Salari and Ortega [8]. Individual truck data are presented in the left plot and the platoon-average data in the right plot (symbols are experimental data and lines are model predictions).

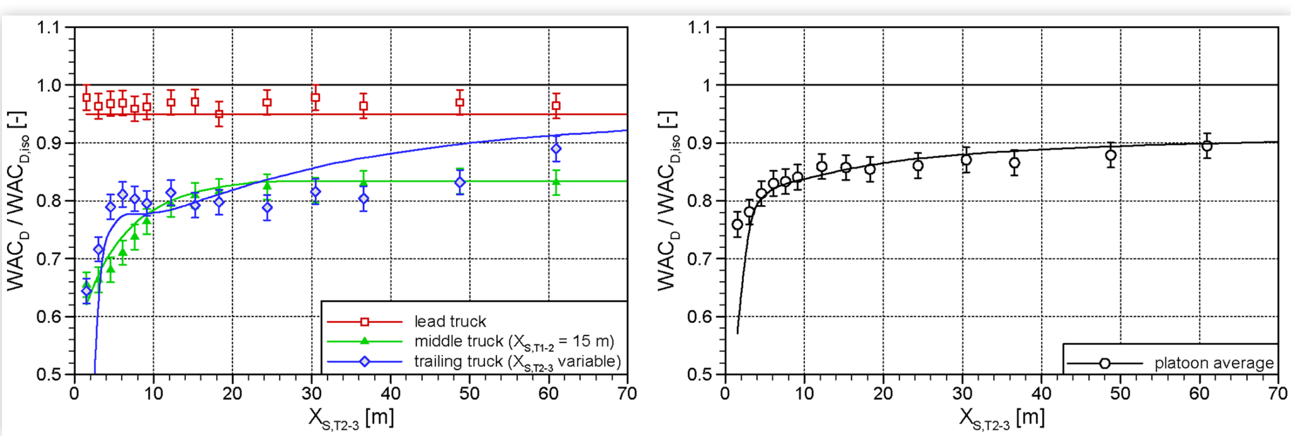

© National Research Council Canada

under-prediction of the platooning benefit in the 25 m to 50 m range. This is attributed to a similar under-prediction at higher yaw angles that was observed with the 1/15-scale two-truck data in Figure 8. As described earlier, this may be due to a model deficiency or may be due to wider wakes associated with interactions of the wakes with the wind-tunnel boundary layer. Regardless of the cause, the model as presented here provides a reasonable representation of the trends and magnitudes of platoon drag reduction. The right plot in Figure 10, which shows the platoon-averaged results, shows good agreement at all but the smallest separation distance of 1.5 m.

Cab-over Simulations

Since its initial development based on North-American-style tractor-trailer combinations, adaptations were made to the model to account for cab-over-style trucks that are prevalent in many regions of the world. These adaptation, noted in earlier sections describing base and wake-effect drag-reduction models, are based on a single data set, that of Törnell et al. [2], of high-fidelity CFD results for no-cross-wind conditions. These adaptations should, therefore, be taken as proposed adaptations that require additional validation.

Figure 11 presents the predictions for the drag-area values of the lead and trailing trucks, compared to the values visually-extracted from [2]. The model, which was tuned for these specific data, show good agreement for both lead and trailing trucks only for separation distances of 5 m and larger. As described by Törnell et al., the 2.5 m condition shows significant changes to the inter-vehicle flow structure compared to larger separation distances. Similar changes in flow structure at small distances may be the cause for poor model performance against some of the sub-5mlong-nose-truck configurations discussed in the previous sections. Such results indicate that a close-distance limit on the validity of the current model should be defined, likely in the 3 m to 5 m range.

FIGURE 11 Model predictions of drag area for cab-over-truck-simulation data of [2] at 0° yaw angle.

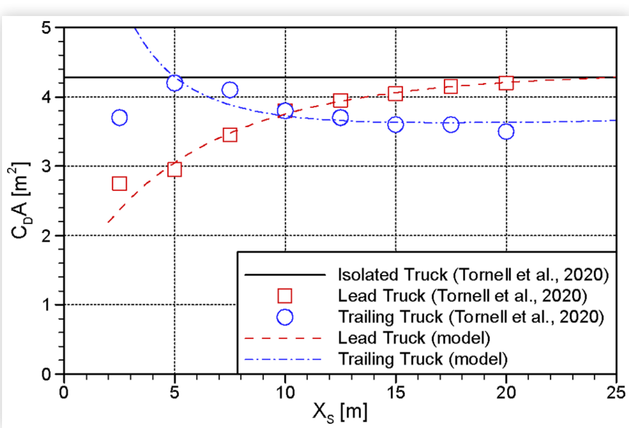

© National Research Council Canada

Conclusions

A physics-guided empirical model for predicting the drag reduction associated with truck platooning was developed and described in this paper. Based on the aerodynamic-drag performance of the isolated-truck and the geometry of the vehicles and platoon formation, the model predicts the influence of longitudinal separation distance, lateral offset, vehicle shape/type, and cross winds on the base-drag-reduction and wake-effect-drag-reduction contributions of the platooning phenomena. Validation of the model was documented via comparison to three experimental data sets (wind-tunnel and track studies) and a high-fidelity simulation data set, showing good agreement in predicting the drag reduction magnitudes and trends for separation distances as small as about 5 m and as large as about 80 m, and for yaw-angle magnitudes as large as 15°. Based on these validations, the model is expected to be valid for heterogeneous platoons with large numbers of dissimilar trucks. Some discrepancies were noted between predictions and wind-tunnel data at some higher yaw angles and at larger separation distances, which may be associated with the static-ground-plane wind-tunnel arrangements. A minimum-distance limit of 3 m is recommended for use of the model. The model is recommended for use with long-nose North-American-style trucks, with additional validation required for cab-over style trucks, particularly in cross-wind scenarios.

Acknowledgements

The author would like to thank Kambiz Salari and Jason Ortega of the Lawrence Livermore National Laboratory for providing access to the 1/50-scale wind-tunnel measurements that were used to support the development of the model, some of which are reproduced in Figure 10.

The work presented in this paper was funded by Transport Canada's ecoTECHNOLOGY for Vehicles program. The views and opinions of the authors expressed herein do not necessarily state or reflect those of Transport Canada.

References

1. McAuliffe, B.R. and Ahmadi-Baloutaki, M., "A Wind-Tunnel Investigation of the Influence of Separation Distance, Lateral Stagger, and Trailer Configuration on the Drag-Reduction Potential of a Two-Truck Platoon," *SAE Int. J. Commer. Veh.* 11, no. 2 (2018): 125-150, doi:10.4271/02-11-02-0011.
2. Törnell, J., Sebben, S., and Söderblom, D., "Influence of Onter-Vehicle Distance on the Aerodynamics of a Two-Truck Platoon," *International Journal of Automotive Technology* 22, no. 3 (2021): 747-760, doi:10.1007/s12239-021-0068-5.

3. Sun, X., Wu, H., Abdolmaleki, M., Yin, Y. et al., "Investigating the Potential of Truck Platooning for Energy Savings: Empirical Study of the U.S. National Highway Freight Network," *Transportation Research Record* 2675, no. 12 (2021): 784-796, doi:10.1177/03611981211031231.
4. Han, Y., Kawasaki, T., and Hanaoka, S., "The Benefits of Truck Platooning with an Increasing Market Penetration: A Case Study in Japan," *Sustainability* 14 (2022), doi:10.3390/su14159351.
5. Taylor, A.H., Droege, M.J., Shaver, G.M., Sandoval, J.A. et al., "Capturing the Impact of Speed, Grade, and Traffic on Class 8 Truck Platooning," *IEEE Transactions on Vehicular Technology* 69, no. 10 (2020), doi:10.1109/TVT.2020.3009489.
6. Tadakuma, K., Doi, T., Shida, M., and Maeda, K., "Prediction Formula of Aerodynamic Drag Reduction in Multiple-Vehicle Platooning Based on Wake Analysis and on-Road Experiments," *SAE Int. J. Passeng. Cars - Mech. Syst.* 9, no. 2 (2016), doi:10.4271/2016-01-1596.
7. Schmid, M., Liu, D., Eksioglu, B., Huynh, N. et al., "Prediction Model for Energy Consumption in Heavy-Duty Vehicle Formations," in: Cromartya, L., Shirwaiker, R. and Wang, P. (Eds), *Proceedings of the 2020 IISE Annual Conference*, (2020).
8. Salari, K. and Ortega, J., "Experimental Investigation of the Aerodynamic Benefits of Truck Platooning," SAE Technical Paper 2018-01-0732 (2018), doi:10.4271/2018-01-0732.
9. Lammert, M.P., McAuliffe, B.R., Raeesi, A., Smith, P. et al., "Impact of Lateral Alignment on the Energy Savings of a Truck Platoon," SAE Technical Paper 2020-01-0594 (2020), doi:10.4271/2020-01-0594.
10. Sujan, V.A., Jones, P., and Siekmann, A., "Heavy Duty Commercial Vehicle Platooning Energy Benefits for Conventional and Electrified Powertrains," 2022 International Conference on Connected Vehicle and Expo (ICCVE) Paper 978-1-6654-1687-0/22, IEEE, 2022. doi:10.1109/ICCVE52871.2022.9742749.
11. Ortega, J. and Salari, K., "Experimental Investigation of the Aerodynamic Benefits of Truck Platooning: Two- and Four-Vehicle Platoons," SAE Technical Paper 2021-01-0942 (2021), doi:10.4271/2021-01-0942.
12. McAuliffe, B.R., Ahmadi-Baloutaki, M., Croken, M., and Raeesi, A. "Fuel-Economy Testing of a Three-Vehicle Truck Platooning System," NRC Report LTR-AL-2017-0008, 2017.
13. McAuliffe, B.R., Lammert, M., Lu, X., Shladover, S. et al., "Influences on Energy Savings of Heavy Trucks Using Cooperative Adaptive Cruise Control," SAE Technical Paper 2018-01-1181 (2018), doi:10.4271/2018-01-1181.
14. McAuliffe, B.R., Raeesi, A., Lammert, M.P., Smith, P. et al., "Impact of Mixed Traffic on the Energy Savings of a Truck Platoon," *SAE Int. J. Advances & Curr. Prac. In Mobility* 2, no. 3 (2020): 1472-1496, doi:10.4271/2020-01-0679.
15. McAuliffe, B.R., Smith, P., Raeesi, A., Hoffman, M. et al., "Track-Based Aerodynamic Testing of a Two-Truck Platoon," *SAE Int. J. Advances & Curr. Prac. In Mobility* 3, no. 3 (2021): 1450-1472, doi:10.4271/2021-01-0941.
16. McAuliffe, B.R. and Ahmadi-Baloutaki, M., "An Investigation of the Influence of Close-Proximity Traffic on the Aerodynamic Drag Experienced by Tractor-Trailer Combinations," *SAE International Journal of Advances and Current Practices in Mobility* 1, no. 3 (2019): 1251-1264, doi:10.4271/2019-01-0648.
17. McAuliffe, B.R., Sowmianarayanan, B. and Barber, H. "Near-to-Far Wake Characteristics of Road Vehicles Part 1: Influence of Ground Motion and Vehicle Shape." *SAE Int. J. Advances & Curr. Prac. In Mobility* 3(4): 2009-2024, doi:10.4271/2021–01–0957, 2021.
18. McAuliffe, B.R., Sowmianarayanan, B. and Barber, H. "Near-to-Far Wake Characteristics of Road Vehicles Part 2: Influence of Cross Winds and Free-Stream Turbulence." *SAE Int. J. Advances & Curr. Prac. In Mobility* 3(4): 2046-2068, doi:10.4271/2021–01–0949, 2021.
19. McAuliffe, B.R. and Barber, H., "Simulating Traffic-Wake Effects in aWind Tunnel," *SAE Int. J. Advances & Curr. Prac. In Mobility* (2023), doi:10.4271/2023-01-0950.
20. Eskridge, R.E. and Thompson, R.S., "Experimental and Theoretical Study of the Wake of a Block-Shaped Vehicle in a Shear-Free Boundary Flow," *Atmospheric Environment* 16, no. 12 (1982): 2821-2836.
21. Golsch, K., Duncan, B., and Kandasamy, S., "Improved CFD Methodology for Class 8 Tractor-Trailer Coastdown Correlation," SAE Technical Paper 2013-01-2412 (2013), doi:10.4271/2013-01-2412.
22. SAE J1252, "SAE Wind Tunnel Test Procedure for Trucks and Busses," *Surface Vehicle Recommended Practice J 1252* (2012).

Nomenclature

Symbols:

A - Frontal area [m^2]

AR - Aspect ratio [-]

B - Wake-shape constant [-]

C_D - Drag-force coefficient [-]

H - Vehicle height [m]

L - Vehicle length [m]

N - Number of vehicles [-]

N_T - Number of truck in a platoon [-]

R_{WO} - Wake-offset ratio [-]

SF - Scaling factor [-]

U - Wind speed [m/s]

X_S - Separation distance [m]

X_{ext} - Separation-distance extension [m]

y - Lateral coordinate [m]

Y_{off} - Lateral offset [m]

α - Wake-spreading-rate constant [-]

γ - Wake-width constant [-]

Δ - Difference value [-]
η - Normalized lateral coordinate [-]
Λ - Wake-strength constant [-]
ψ - Yaw angle [°] or [rad]

Subscripts:
0 - Zero-yaw-angle value
avg - Average value
base - Parameter associated with HDV base
DV - Dry-van value
eff - Effective value
fs - Freestream value
i - Index value
j - Index value
meas - Based on measured value
min - Minimum value
near - Near-wake value
n - Platoon-location index
near - Nearby or close-distance value
off - Offset value
ref - Reference value
wd - Wake-deficit value
ψ - Yaw-angle value

© 2024 National Research Council Canada; Published by SAE International. This Open Access article is published under the terms of the Creative Commons Attribution License (http://creativecommons.org/licenses/by/4.0/), which permits distribution, and reproduction in any medium, provided that the original author(s) and the source are credited.

Positions and opinions advanced in this work are those of the author(s) and not necessarily those of SAE International. Responsibility for the content of the work lies solely with the author(s).

e-ISSN 2641-9645